ELSEVIER

Journal of Photochemistry and Photobiology
A: Chemistry 89 (1995) 141–146

Journal of PHOTOCHEMISTRY AND PHOTOBIOLOGY A: CHEMISTRY

Intramolecular excimer formation from 1,8-*N*-alkyldinaphthalimides

T.C. Barros [a], P. Berci Filho [b], V.G. Toscano [a], M.J. Politi [a,*]

[a] *Instituto de Química, Universidade de São Paulo, São Paulo, Brazil*
[b] *Instituto de Química de São Carlos, Universidade de São Paulo, São Paulo, Brazil*

Received 16 November 1994; accepted 10 January 1995

Abstract

Conjugation of π electrons between imide groups vicinal to arene moieties can drive the photophysical and photochemical properties to a mixed transition of close lying states having n,π^* and π,π^* characters (Almeida et al., *J. Photochem. Photobiol. A: Chem., 58* (1991) 289). Furthermore, the extent of mixing between these states is a function of the molecular geometry (Barros et al., *J. Photochem. Photobiol. A: Chem., 76* (1993) 55). New imides were prepared (1,8-*N*-propyldinaphthalimide (C_3) and 1,8-*N*-butyldinaphthalimide (C_4)) to investigate the n,π^* and π,π^* conjugative effects through space. The steady state and time-resolved fluorescence emission of C_3 and C_4 in solvents of high polarity shows the presence of a new emitting species at longer wavelength. This emission arises from a rotation in the alkyl chain, resulting in an intramolecular energy transfer between the two chromophores during the excited state lifetime of the extended form.

Keywords: Intramolecular excimer formation; Naphthalimide dimers; Intramolecular excimer decays; Bisnaphthalimides excimers; Naphthalide diimides

1. Introduction

Although the photophysical and photochemical properties of phthalimides are due to the n,π^* character of their lowest singlet excited state, for *N*-alkylphthalimides (NAP), the fluorescence quantum yield as a function of the solvent polarity parameters indicates a decrease in the energy of the π,π^* transition, therefore rendering a mixed (n,π^*)(π,π^*) character for the lowest unoccupied molecular orbital (LUMO) state in high polarity medium [1].

By increasing the density of π states susceptible to conjugation with the imide moiety, as in naphthalimides, the π,π^* emission can overwhelm that of n,π^*, leading the LUMO state to a mostly pure π,π^* character [2,3]. Interestingly for 2,3- and 1,2-naphthalimides, the n,π^* character still prevails, whereas for 1,8- naphthalimide, geometrical constraints favour the π,π^* transition [4,5].

In order to analyse the effect through space of increased π,π^* energy density, we prepared 1,8-dinaphthalic dimers, having the two chromophores connected via σ bonds (propyl and butyl, Scheme 1). It is shown that, depending on the solvent polarity, a condensed configuration for the dimer in the excited state is favoured, resulting in an excimer fluorescence emission.

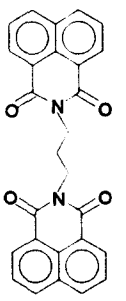

1,8-N-propyldinaphthalimide

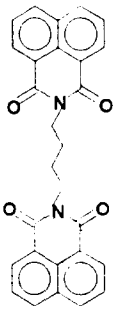

1,8-N-butyldinaphthalimide

Scheme 1.

2. Experimental section

2.1. Materials

2.1.1. 1,8-Naphthalimide

1,8-Naphthalic anhydride (Aldrich PA) (0.1 mol) was refluxed for about 4 h in a large molar excess of ammonium hydroxide (200 times) [6]. The precipitated

* Corresponding author.

SSDI 1010-6030(95)04040-4

product was washed three times with cold water and dried under low pressure. The product was identified by elemental analysis, IR and proton nuclear magnetic resonance (^{1}H NMR) spectroscopy.

2.1.2. 1,8-Naphthalimide potassium salt

1,8-Naphthalimide and ethanolic KOH (in equimolar concentrations) were stirred in warm dried ethanol until quantitative precipitation [7]. The product was washed with cold ethanol and dried under low pressure. The material was characterized by elemental analysis.

2.1.3. 1,8-N-Propyldinaphthalimide (C_3) and 1,8-N-butyldinaphthalimide (C_4)

Diimides C_3 and C_4 were prepared by refluxing 1,8-*N*-naphthalimide potassium salt with 1,3-dibromopropane or 1,4-dibromobutane (molar ratio, 2.2 : 1.0) in *N,N*-dimethylformamide (DMF) for about 25 h. The reaction was followed by thin layer chromatography (TLC) using dichloromethane–ethyl ether (48 : 2) as eluent. The precipitates were washed with cold DMF and dried under low pressure. C_4 was recrystallized from cold dichloromethane–ethyl ether (5 : 1 (v/v)) or hot dichloromethane (2 : 1 (v/v)). Both diimides were characterized by elemental analysis, IR and ^{1}H NMR spectra. C_3 and C_4 ^{1}H NMR chemical shifts are listed in Table 1.

The other reagents employed were PA grade and the organic solvents were distilled.

2.2. Methods

UV–visible absorption spectra were recorded on a Beckman DU-7 or a Hitachi U-2000 spectrophotometer. Fluorescence measurements were carried out in an LS-1 (PTI-Canada) spectrofluorometer. Steady state fluorescence emission spectra were computer corrected. Fluorescence quantum yields (Φ_f) were calculated relative to the area of the corrected emission spectrum of quinine bisulphate (QBS) in $HClO_4$ (0.1 N) ($\Phi_f = 0.546$) [8]. Absorbances for Φ_f determination were in the 0.01–0.02 range. Fluorescence decay measurements and time-resolved fluorescence emission spectroscopy (TRES) were performed in the same machine.

Table 1
^{1}H NMR chemical shifts for 1,8-*N*-propyldinaphthalimide (C_3) and 1,8-*N*-butyldinaphthalimide (C_4) in $CDCl_3$

C_3	δ (ppm)	C_4	δ (ppm)
CH (t-Ar)	7.7	CH (t-Ar)	7.8
CH (d-Ar)	8.2	CH (d-Ar)	8.2
CH (d-Ar)	8.5	CH (d-Ar)	8.6
CH_2 (t-αN)	4.4	CH_2 (t-αN)	4.3
CH_2 (q-βN)	2.2	CH_2 (m-βN)	1.9

Two distinct approaches were employed for TRES. In the first, gated TRES (GTRES), the time basis in the LS-1 spectrofluorometer was gated at different times relative to the impulse signal (lamp) and the fluorescence intensity was recorded as the emission monochromator was scanned. In the second, standard TRES (STRES), fluorescence intensity decays were monitored at distinct wavelengths and, after scanning the desired region, a TRES graph was computer built. In the first experimental approach, the buildup and decay of transients are easier to observe, whereas with the second approach, rates can be software deconvoluted. Thyratron-driven light pulses were obtained from an arc lamp filled with extra pure N_2 and operated at 337 nm (delivering pulses of approximately 8 ns full width at half-maximum (FWHM)). Lifetimes were obtained by standard deconvolution routines.

3. Results

The UV–visible absorption spectrum of C_3 (Fig. 1) is similar to that of the monomer of 1,8-*N*-butylnaphthalimide (αNBN). The molar extinction coefficient maximum (ϵ) for C_3 and C_4 is 32 000 M^{-1}, which is about twofold larger than that of αNBN ($\epsilon = 14\,000$ M^{-1}) [4], suggesting no ground state interaction between the two chromophore rings.

The fluorescence emission maximum (approximately 390 nm) shows, as for αNBN [4], a small bathochromic shift and the appearance of vibronic shoulders with decreased medium polarity (Fig. 2). The emission spec-

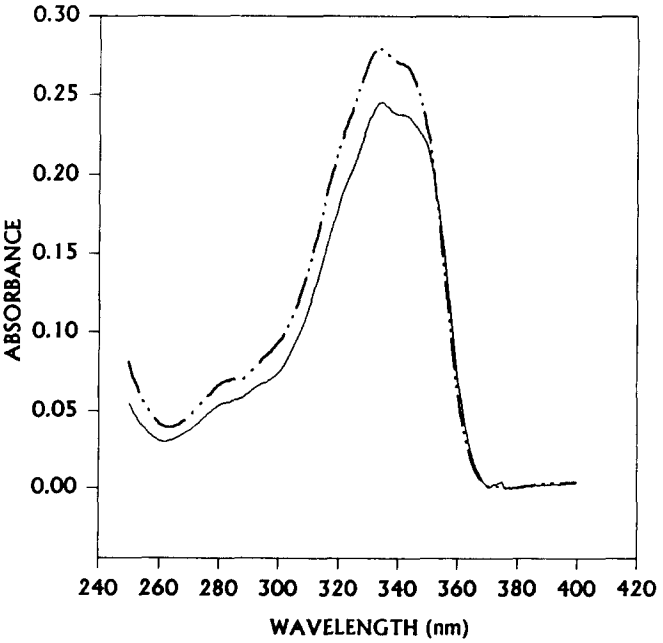

Fig. 1. Absorption spectra of 1,8-*N*-butylnaphthalimide (–··–) and 1,8-*N*-propyldinaphthalimide (full line) in ethanol (approximately 2.0×10^{-5} and 0.9×10^{-5} M respectively).

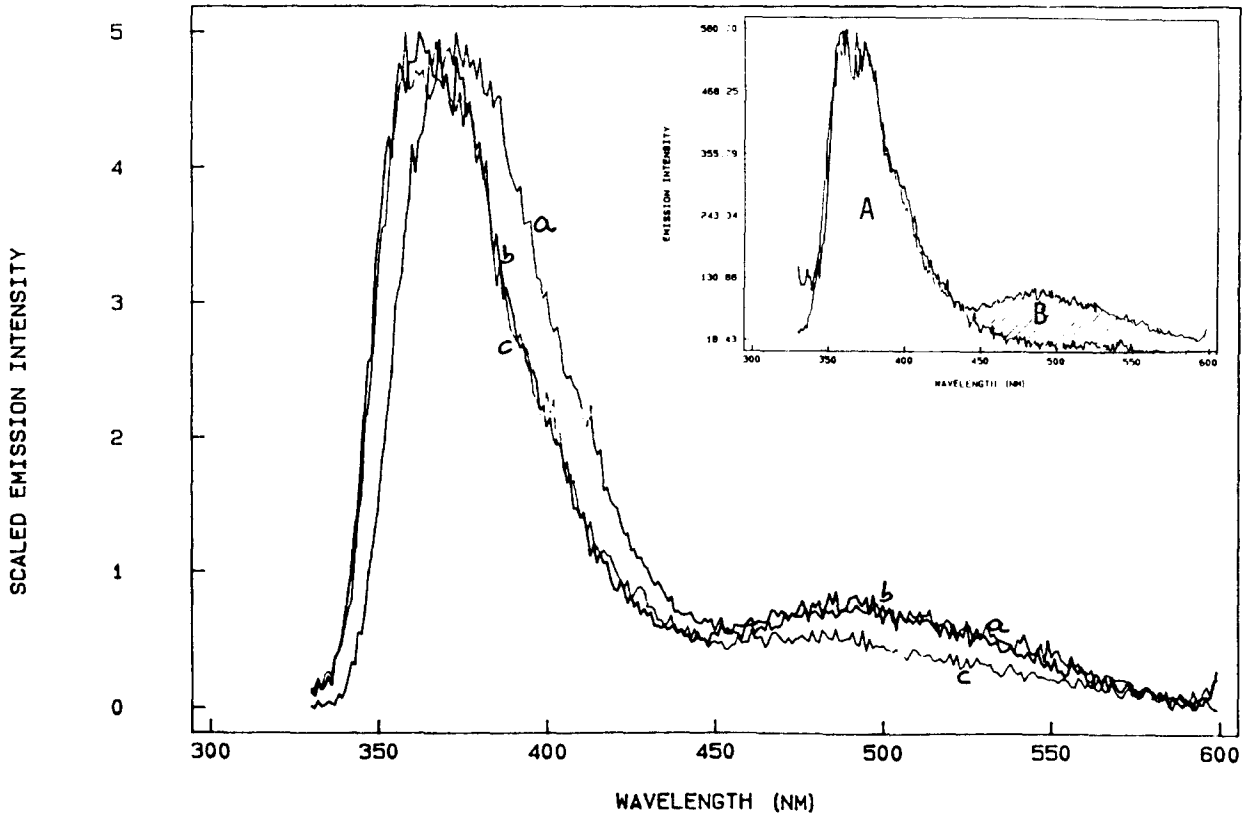

Fig. 2. Corrected fluorescence emission spectra of 1,8-*N*-propyldinaphthalimide (C_3) in methanol (a), CH_3CN (b) and CH_2Cl_2 (c). Inset: superimposition of 1,8-*N*-propyldinaphthalimide (C_3) and 1,8-*N*-butylnaphthalimide (αNBN) normalized emission spectra in CH_3CN. Areas labelled A and B correspond to the monomer and excimer respectively.

tra of both diimides in solvents of high polarity, such as methanol and acetonitrile, present an extra band of lower intensity around 480 nm (Fig. 2). For αNBN, up to approximately 2×10^{-3} M in methanol, this band is not observed.

In order to determine the origin of the emission at 480 nm, GTRES data (see Section 2.2) were collected. Fig. 3 presents the normalized gated time-resolved fluorescence emission spectra of C_3 in methanol. It can be observed that during the first 5–6 ns (spectra a to c, Fig. 3) only the emission at 390 nm is significant. After this delay, the emission at 480 nm starts to increase (spectra d to g, Fig. 3). It is important to note that the spectra in this figure were normalized given the larger intensity of the high energy emission (cf. Fig. 2). Consequently, the time dependence of the emission at 480 nm on that at 390 nm is not clear by this method.

On the other hand, STRES (see Section 2.2) shows clearly the kinetic interdependence between the 390 and 480 nm emission bands (Fig. 4). The buildup in the fluorescence intensity in the 480 nm region up to approximately 6 ns and its subsequent slow decay can be observed. Clearly, the overlap of the 390 and 480 nm emission is quite high; consequently, the transient buildup in the 480 nm region appears as a shoulder in the main emission. The time-resolved fluorescence emission spectra at lower wavelengths show only a monotonic decay.

In Fig. 5, the fluorescence emission decays of C_4 in methanol at 390 nm (A) and 490 nm (B) are presented. In this figure, line a is the lamp, line b is the sample decay and line c is the best fitted decay (monoexponential or biexponential, see Table 2). The decay is obviously very fast and almost within the nominal limit of our apparatus (approximately 0.1 ns). It is important to note, however, that the lamp signal (scatter) was observed at 337 nm, whereas the contribution due to scattered light was negligible at 390 nm (the fluorescence emission). The decay at this wavelength could be fitted well to a monoexponential function with a lifetime (τ) of approximately 1.0 ns (Fig. 5(A) and Table 2). The observed decay at 490 nm, however, is not a single exponential (Fig. 5(B)). In Table 2, the decay parameters at selected wavelengths are presented. For both C_3 and C_4, the decay is a sum of exponentials above 460 nm. The decays observed at 480 and 520 nm are not equivalent, a feature which can be understood on the basis of the large contribution of the 390 nm emission in the 480 nm region and its lack of contribution at 520 nm (see Fig. 4 for example). Accordingly meaningful

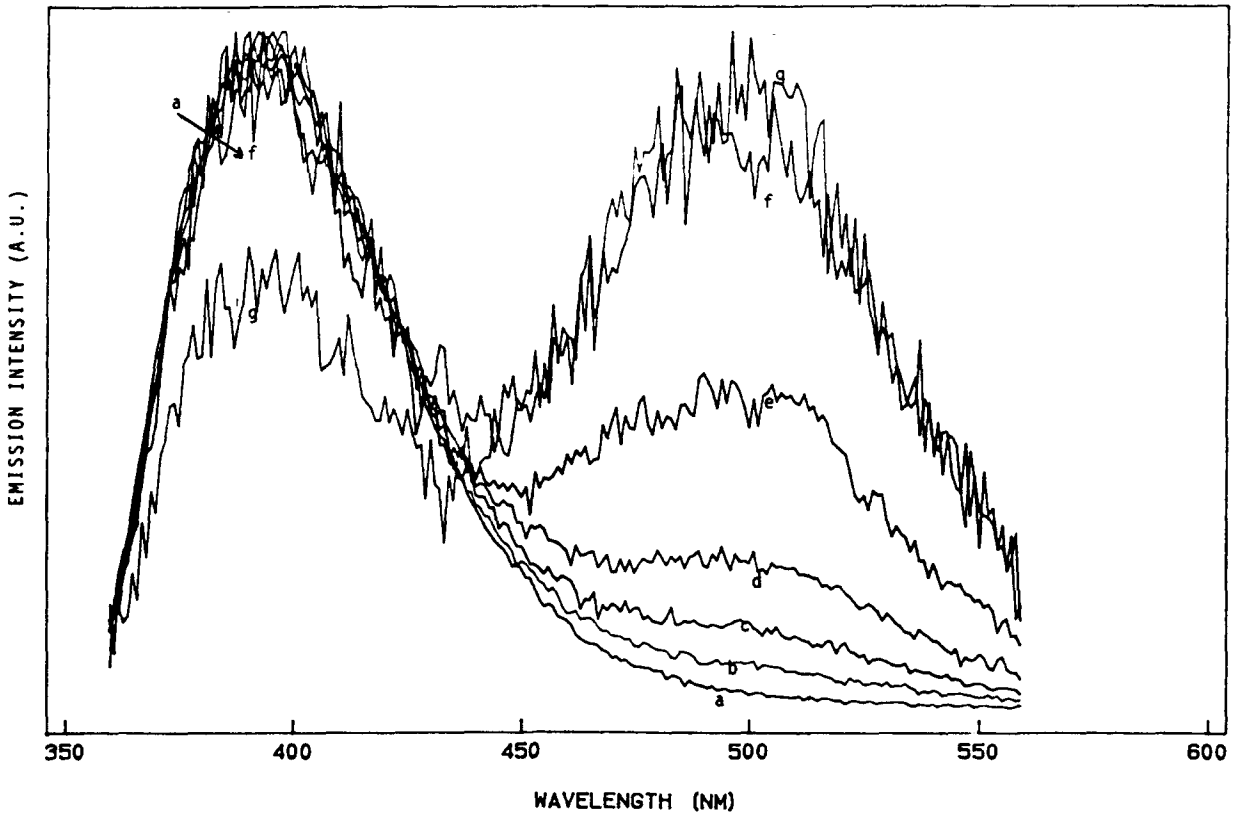

Fig. 3. Gated time-resolved emission spectra of 1,8-*N*-propyldinaphthalimide in methanol (normalized intensities): (a) 1 ns before the lamp pulse and 2 ns (b), 5 ns (c), 7 ns (d), 10 ns (e), 13 ns (f) and 28 ns (g) after the lamp pulse.

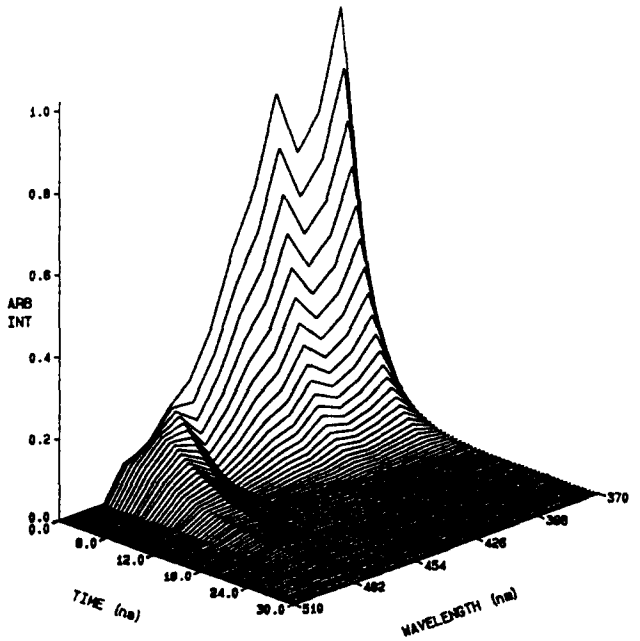

Fig. 4. Standard time- resolved emission spectra of 1,8-*N*-propyldinaphthalimide in methanol.

data, that are independent of band overlap, were analysed only at the longer wavelength.

4. Discussion

Resonance energy transfer in the form of orbital energy mixing or excimer emission constitutes one of the main routes in an attempt to build convenient molecular wires [9,10]. In this regard, naphthalimides are good candidates, providing the interplay of n,π^* and π,π^* transition mixing [4]. In this study, our objective was to promote mixing via spatial conjugation among methylene-linked (C_3 and C_4) chromophores. The data presented show the appearance of a new emitting species at lower energy for both diimides in solvents of relatively high polarity (Fig. 2). The emission at longer wavelength is shown to be kinetically dependent on that at high energy (Figs. 3 and 4). A fast decay at approximately 390 nm (1 ns) gives rise to a fluorescence emission buildup at approximately 480 nm (5 ns), followed by a relatively long-lived decay (approximately 25 ns) (Table 2). The spectral independence of the two linked chromophores on the UV–visible absorption spectra (Fig. 1) should also be noted. This behaviour is consistent with intramolecular excimer formation, as proposed by Zachariasse [11] for covalently linked pyrenes and represented in Scheme 2 where k_a and k_d are the rate constants leading to the condensed A*A or extended A*——A molecule, and τ represents the associated lifetime. Therefore, in this presentation, k_a represents

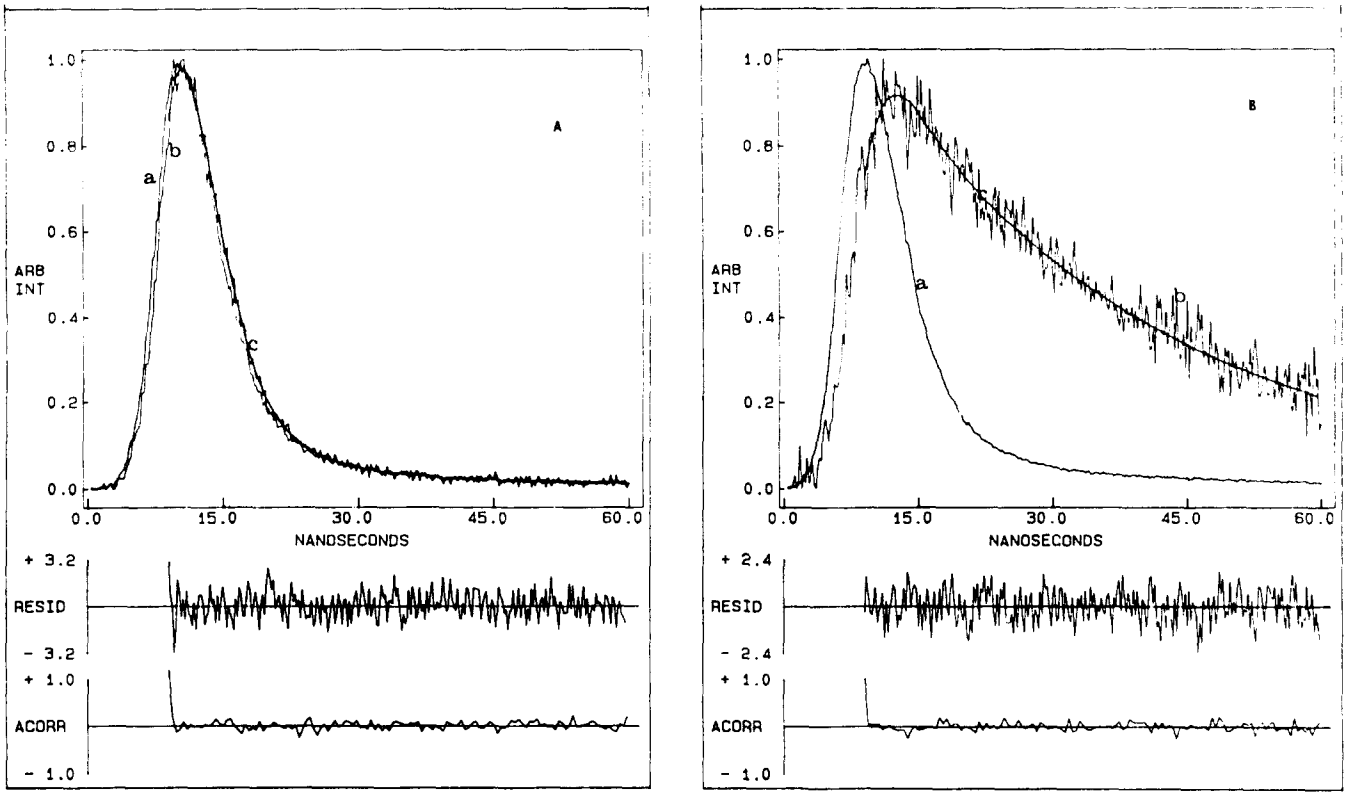

Fig. 5. Fluorescence decay of 1,8-*N*-butyldinaphthalimide in methanol at $\lambda = 380$ nm (A) and $\lambda = 480$ nm (B) with excitation at 337 nm (line a is the lamp, line b is the sample decay and line c is the best fitted function).

Table 2
Fluorescence decay parameters of 1,8-*N*-propylnaphthalic (I) and 1,8-*N*-butylnaphthalic (II) dimers in methanol

Dimer	λ (nm)	A_1	τ_1 (ns)	A_2	τ_2 (ns)
I	380	1.00	0.97	–	–
I	480	0.83	1.29	0.16	26.87
I	520	−0.33	0.64	1.00	22.89
II	380	1.00	1.02	–	–
II	480	0.85	1.30	0.15	28.28
II	520	−3.36	1.02	1.00	22.54

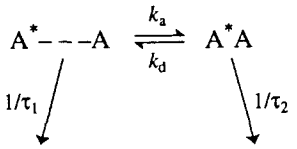

Scheme 2.

the sum of the rotational contributions (solvent polarity dependent) which lead to the juxtaposition of the two imide rings in an appropriate geometry and result in excimer emission (approximately 480 nm). Before analysing the kinetic aspects resulting from Scheme 2, the emission quantum yields (Φ_f) for the extended and condensed forms were assessed by deconvoluting the emission spectra (Fig. 2) using that of a pure monomeric naphthalimide (αNBN) (i.e. assuming that the extended molecule behaves as the free monomer). This approach is represented in Fig. 2 (inset) where the normalized emission due to the monomer and that due to the extended diimide are superimposed. The areas under the spectra were calculated and transformed into Φ_f relative to QBS emission [8]. In Table 3, the calculated yields are presented. It is clear that the overall yield

Table 3
Fluorescence quantum yields (Φ_f) of 1,8-*N*-propylnaphthalic (I) and 1,8-*N*-butylnaphthalic (II) dimers and 1,8-*N*-butylnaphthalimide (αNBN)

Compound	Solvent	Quantum yield (Φ_f)	
		Monomer [a]	Excimer [a]
I	MeOH	0.040	0.010
I	CH_3CN	0.020	0.005
I	CH_2Cl_2	0.011	0.002
II	MeOH	0.042	0.009
II	CH_3CN	0.015	0.005
II	CH_2Cl_2	0.008	0.002
αNBN	MeOH	0.082 [b]	
αNBN	CH_3CN	0.063	
αNBN	CH_2Cl_2	0.047	

[a] Φ_f was calculated from the superimposition of the area of the free monomer (αNBN) on the total area (see inset, Fig. 2).
[b] Ref. [4].

for αNBN is larger than that of the diimides in the three solvents studied, the Φ_f values decrease with decreasing solvent polarity (as observed for αNBN) and the excimer and overall yield increase with increasing polarity.

The fluorescence decay functions for both excimer and monomer can be fitted by sums or differences of two exponentials as

$$i(t) = A_1 \exp(-\Lambda_1 t) + A_2 \exp(-\Lambda_2 t) \quad (1)$$

The decay parameters Λ_1 and Λ_2, corresponding to $1/\tau_1$ and $1/\tau_2$ respectively, were determined from statistical analysis of the response functions adjusted to the experimental data at each wavelength (Table 2).

Eq. (1) fits the formation of an intramolecular excited state dimer following the equilibria described in Scheme 2. Using the approach suggested by Zachariasse and Kühnle [12] and Birks [13], we can estimate, as a first approximation for the data in Table 2 ($\lambda = 520$ nm), values for k_a and k_d in the range 1×10^8–10^{10} s^{-1} and 1×10^7–10^9 s^{-1} respectively, depending on the lifetimes chosen for the monomer and excimer. Independent of their accuracy, k_a is larger than k_d by about one order of magnitude in agreement with the relatively long-lived emission at lower energy.

Our findings can be rationalized in terms of σ bond rotation during the excited state, leading to close facing of the two chromophores and energy transfer. This process is favoured in solvents of relatively high polarity in which the two rings are close, but still electronically independent; fast rotation through σ bond leads to a condensed format and on excitation, excimer formation.

Studies in progress with more appropriate equipment (10 ps time resolution) will allow more detailed kinetic information to be obtained. This will enable the mechanism for intramolecular excimer formation presented here to be determined more accurately.

Acknowledgments

This work was supported by grants from the Brazilian Agencies Fundação de Amparo à Pesquisa do Estado de São Paulo (Fapesp), Financiadora de Estudos e Projetos (Finep) and Conselho Nacional de Pesquisa (CNPq).

References

[1] P. Berci Filho, V.G. Toscano and M.J. Politi, *J. Photochem. Photobiol. A: Chem., 43* (1988) 51.
[2] F.C.L. Almeida, V.G. Toscano, O. Santos, M.J. Politi, M.G. Newman and P. Berci Filho, *J. Photochem. Photobiol. A: Chem., 58* (1991) 289.
[3] P.H. Mazzocchi, in A. Padwa (ed.), *Organic Photochemistry*, Vol. 5, Marcel Dekker, New York, 1981, p. 421.
[4] T.C. Barros, G.R. Molinari, P. Berci Filho, V.G. Toscano and M.J. Politi, *J. Photochem. Photobiol. A: Chem., 76* (1993) 55.
[5] V. Wintgens, P. Valat, J. Kossanyi, L. Biczok, A. Demeter and T. Bérces, *J. Chem. Soc., Faraday Trans., 90* (3) (1994) 411.
[6] G.F. Jaubert, *Ber., 28* (1895) 360.
[7] A.M. Mattocks and O.S. Hutchison, *J. Am. Chem. Soc., 70* (1948) 3474.
[8] J.N. Miller (ed.), *Standards in Fluorescence Spectrometry*, Vol. 2, Ultraviolet Spectrometry Group, Chapman and Hall, New York, 1981.
[9] V. Balzani and F. Scandola, *Supramolecular Photochemistry*, Ellis Horwood, 1991.
[10] J.N. Onuchic and D.N. Beratan, *J. Am. Chem. Soc., 109* (1987) 6771.
[11] K.A. Zachariasse, G. Duveneck and W. Kühnle, *Chem. Phys. Lett., 113* (4) (1985) 337.
[12] K.A. Zachariasse and W. Kühnle, *Z. Phys. Chem., 101* (1976) 267.
[13] J.B. Birks, *Photophysics of Aromatic Molecules*, Wiley-Interscience, New York, 1969.